Proceeding of the National Conference
On Undergraduate Research (NCUR) 2009
University of Wisconsin-La Crosse
La Crosse, Wisconsin
April 16-18, 2009

The Non-Linear Cantilever: A Graphical User Interface

Abner Ortiz and Greichaly Cabrera
Department of Mathematics
University of Puerto Rico at Humacao
Humacao, PR 00791-4300

Faculty Advisor: Pablo V. Negrón

Abstract

The cantilever problem consists of studying the deformations of a bar or rod that is attached to a wall on one end and is subjected to a torque or applied force on the other end. In the classical cantilever problem, the constitutive functions (the functions characterizing the material that composes the bar) are linear, the material of the bar is homogeneous, inextensible and unshearable; there is no applied torque, and the applied force is vertical. The classical problem was studied by Jas. Bernoulli (1694) and L. Euler (1727). The cantilever problem still has many applications in engineering, and more recently in nano technology. This project is considering a nonlinear model of the cantilever in which the material of the bar is non-homogeneous, extensible and shearable. The nonlinear model is introduced to describe a finite difference numerical scheme for computing approximate solutions of the problem. The resulting nonlinear system of equations is solved with Newton's method, by taking advantage of the structure of the Jacobian matrix (almost tridiagonal) to solve the intermediate linear systems efficiently. Moreover it has been developed a graphical user interface which allowed us to experiment with the model and to control more effectively the different constitutive and force parameters. These tools are used to study the dependence of the bar deformations on thickness variations and the different constitutive parameters and applied forces. Also, this helps in the study of the severity or magnitude of the shear strain as the parameters and forces are changed.
Keywords: Nonlinear Cantilever, GUI

1. Introduction

We consider the problem of finding the shape that assumes a bar composed of a certain material, when it is attached to a wall, and we apply some force or torque on the other end. This problem is known as the *cantilever*. In the classical problem of the cantilever (Bernoulli, 1694; Euler, 1727), the functions that describe the material composing the bar (*constitutive functions*) are assumed to be linear. In this paper we consider nonlinear constitutive functions for the material behavior that include effects for shear, bending, and torsion.[1] For simplicity it is assumed that the cross sections of the bar are circular (see Figure 1).

The problem of the cantilever has many applications in engineering in particular for the construction of bridges. It has also become important in the field of nano science or technology as some deformations of nano fibers can be described very well with a model of a cantilever.[3, 4] An interesting problem would be to compare the results of using the models in this paper based on macro mechanical behaviors, with models of deformations of these nano fibers based on molecular dynamics.

The computer simulations performed nowadays in many areas of modern science use what is known as a *graphical user interface* or GUI. The GUI helps the data entry to the computational module which performs the required computations with the values entered by the user. The computational package MATLAB™ provides several tools to create the graphical user interfaces. Using these tools we constructed a GUI for the non-linear cantilever problem that allowed us to systematically change mechanical and constitutive parameters, and then generate different types of deformations.

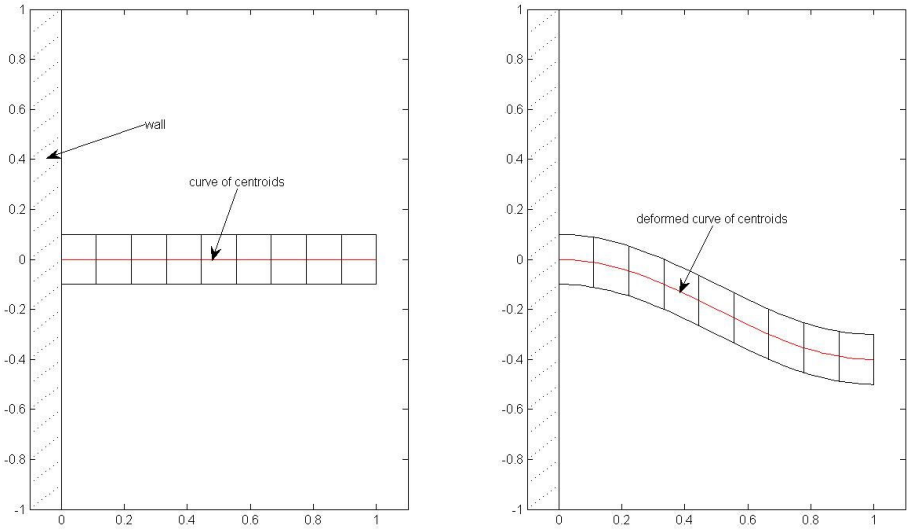

Figure 1: Reference and deformed configurations of the bar.

2. The Mathematical Model

In the Cosserat's special theory, [1] a planar configuration of a column can be described with two functions **r, b**: [0,1]→ span{**i, j**}. The unit vector **b**(s) is called the *directrix* at *s*. If we define the unit vector **a** = **- k** × **b**, then **a, b** belong to span{**i,j**}. Hence there exists a function θ(s) such that:

$$\mathbf{a}(s) = \cos\theta(s)\mathbf{i} + \sin\theta(s)\mathbf{j}, \qquad \mathbf{b}(s) = -\sin\theta(s)\mathbf{i} + \cos\theta(s)\mathbf{j}.$$

Since {**a, b**} is a base for span{**i, j**}, we can write:

$$\mathbf{r}'(s) = v(s)\mathbf{a}(s) + \eta(s)\mathbf{b}(s), \tag{1}$$

for some functions v(s), η(s). These functions together with $\mu(s) = \theta'(s)$ are called the *strains* and they completely characterize the deformation of the column. To ensure that the deformation of the bar is not so severe as to make **r** and **b** parallel, we require that $v(s) > 0$, $s \in [0,1]$.

2.1 mechanical behavior

The contact force and torque exerted by the segment [s,1] of the bar on the segment [0,s] are given by **n**(s) and **m**(s), respectively, while the external (body) force and torque per unit length at the point s are given by **f**(s) and **l**(s), respectively. The equations of equilibrium for the deformed bar are now given by[1]:

$$\mathbf{n}'(s) + \mathbf{f}(s) = \mathbf{0}, \qquad \mathbf{m}'(s) + \mathbf{r}'(s) \times \mathbf{n}(s) + \mathbf{l}(s) = \mathbf{0}. \tag{2}$$

Since we are assuming the deformation of the bar is planar, then there exists functions N(s), H(s), M(s) such that

$$\mathbf{n}(s) = N(s)\mathbf{a}(s) + H(s)\mathbf{b}(s), \qquad \mathbf{m}(s) = M(s)\mathbf{k}. \tag{3}$$

2.2 boundary conditions

The boundary conditions at s = 0, 1 can be specified in several ways. We discuss the conditions at the end s = 1 of the bar, the other case being similar. Given the vectors $\mathbf{r}^1$, $\mathbf{n}^1$, we can specify that

$$\mathbf{r}(1) = \mathbf{r}_1, \quad \text{or} \quad \mathbf{n}(1) = \mathbf{n}_1 .. \tag{4}$$

In addition, given $\theta_1, M_1,$ we could have that

$$\theta(1) = \theta_1 \quad \text{or} \quad M(1) = M_1 . \tag{5}$$

The *boundary value problem* for the deformations of the bar is given by (2) together with one of the boundary conditions in (4) and another from (5), and the same for s = 0.

2.3 the equations for the nonlinear cantilever

Suppose that the initial figuration of the bar is like in Figure 1 and that **f**(s) = 0, **l**(s) = 0, for all s in (2). From the first equation in (2) we have that **n**(s) = constant. If at s=1 we have an applied force given by the vector $\mathbf{n}_1 = -\lambda\left(\cos\alpha\,\mathbf{i} + \sin\alpha\,\mathbf{j}\right),$ then, we have that

$$\mathbf{n}(s) = -\lambda\left(\cos\alpha\,\mathbf{i} + \sin\alpha\,\mathbf{j}\right),$$

for all s. It follows now from (3) that

$$N(s) = -\lambda\cos(\theta(s)-\alpha), \quad H(s) = \lambda\sin(\theta(s)-\alpha). \tag{6}$$

One can show now that the second equation in (2) is equivalent to

$$M'(s) + \lambda\left[\nu(s)\sin(\theta(s)-\alpha) + \eta(s)\cos(\theta(s)-\alpha)\right] = 0 . \tag{7}$$

So far the functions *N*(s), *H*(s), *M*(s) have not been specified. We assume that

$$N(s) = \widehat{N}(\nu(s)), \quad H(s) = D\eta(s), \quad M(s) = (EI)(s)\mu(s), \tag{8}$$

where $D > 0$,

$$\widehat{N}(\nu) = A\,\nu^a - B\,\nu^{-a} - A + B, \quad A, B \geq 0, \quad a > 0, \tag{9}$$

and $(EI)(s) > 0$ for all s. The function $(EI)(s)$ contains the information of the geometrical properties of the cross sections of the bar. Using these expressions together with (6) and (7) we can get the functions $\nu(s), \eta(s)$ in terms of $\theta(s)$ and a differential equation for $\theta(s)$:

$$\nu^a(s) = \frac{P(s) + \sqrt{P^2(s) + 4AB}}{2A}, \quad P(s) = -\lambda\cos(\theta(s)-\alpha) + A - B, \quad \eta(s) = \frac{\lambda}{D}\sin(\theta(s)-\alpha), \tag{10}$$

$$\frac{d}{ds}\left[(EI)(s)\frac{d\theta}{ds}(s)\right] + \lambda\left[\nu(s)\sin(\theta(s)-\alpha) + \eta(s)\cos(\theta(s)-\alpha)\right] = 0. \tag{11}$$

The boundary conditions that the bar is attached to a wall on the left side and that a torque is applied on the right side are equivalent to

$$\theta(0) = 0, \qquad \theta'(1) = \gamma, \tag{12}$$

where γ is proportional to the applied torque.

The equations (10), (11) and (12) constitute the boundary value problem for the cantilever. (The case $\alpha = \pi/2, \nu = 1, \eta = 0$ corresponds to the classical cantilever problem.) After solving these equations for the function $\theta(s)$, we have from (1), (10) and $\mathbf{r}(0) = \mathbf{0}$ that the deformed curve of centroids is given by:

$$\mathbf{r}(s) = \left(\int_0^s [v(t)\cos\theta(t) - \eta(t)\sin\theta(t)]dt \right)\mathbf{i} + \left(\int_0^s [v(t)\sin\theta(t) + \eta(t)\cos\theta(t)]dt \right)\mathbf{j}. \tag{13}$$

3. The Numerical Method

The equations (10), (11) and (12), in general, can not be solved in exact or closed form. It is therefore necessary to turn to numerical methods to approximate its solutions. In this section we will describe a *finite difference method* to approximate these solutions.

First we construct a uniform partition of the interval [0, 1] into *n* sub-intervals. Taking *h* = 1/*n* we have that the i-th interval in such a partition is given by $[s_{i-1}, s_i]$, $1 \le i \le n$, where $s_i = ih$, $0 \le i \le n$. We write $s_{i-1/2}$ to represent the mid point of the interval $[s_{i-1}, s_i]$, that is: $s_{i-1/2} = (s_{i-1} + s_i)/2$, $1 \le i \le n$.

Let θ_i represent an approximation of $\theta(s_i)$, $0 \le i \le n$, and v_i, η_i be given by (10) replacing $\theta(s_i)$ with θ_i. We have now by using twice the mid-point rule for approximating derivatives[2], that equation (11) can be approximated by

$$\begin{aligned} F_i \equiv [(EI)(s_{i+1/2})\theta_{i+1} - ((EI)(s_{i+1/2}) + (EI)(s_{i-1/2}))\theta_i + (EI)(s_{i-1/2})\theta_{i-1}] \\ + \lambda h^2 [v_i \sin(\theta_i - \alpha) + \eta_i \cos(\theta_i - \alpha)] = 0, \end{aligned} \tag{14}$$

where $1 \le i \le n-1$. Using an end-point formula for approximating derivatives, we get that the boundary conditions (12) can be approximated with

$$\theta_0 = 0, \quad F_n \equiv 3\theta_n - 4\theta_{n-1} + \theta_{n-2} - 2h\gamma = 0. \tag{15}$$

The equations (14) and (15) now form a system of equations whose solutions represent the values of $\theta_1, \theta_2, \ldots, \theta_n$. These equations can be solved using Newton's method.[2] Already calculated the values of $\theta_1, \theta_2, \ldots, \theta_n$, we can obtain the deformed curve of centroids from (13) after approximating the corresponding integrals using for instance the trapezoidal rule.[2]

The linear system to be solved on each iteration of Newton's method when applied to the system (14), (15), can be solved very efficiently if one takes into account the sparsity of the corresponding matrix. If $\mathbf{F}(\theta) = (F_1, F_2, \ldots, F_n)^t$, where $\boldsymbol{\theta} = (\theta_1, \theta_2, \ldots, \theta_n)^t$ represents the system (14), (15), then performing the corresponding differentiations one gets:

$$\mathbf{F}'(\boldsymbol{\theta}) = \begin{bmatrix} \mathbf{A} & \mathbf{b} \\ \mathbf{c}^t & \beta \end{bmatrix},$$

where $\mathbf{A}$ is an $(n-1)\times(n-1)$ tridiagonal matrix, $\mathbf{b}, \mathbf{c} \in \Re^{n-1}$, and $\beta \in \Re$. One can show now that the corresponding linear system $\mathbf{F}'(\boldsymbol{\theta})\mathbf{w} = \mathbf{h}$ can be solved by solving two tridiagonal $(n-1)\times(n-1)$ systems, plus two additional inner products, that is in $O(n)$ operations.

4. The Graphical User Interface

Using the tools provided by the package MATLAB™, we developed a graphical user interface to experiment with the cantilever problem. The numerical scheme discussed in Section 3 essentially comprises the computational module which is controlled by the GUI. In Figure 2 we show a snapshot of the cantilever GUI. The interface has several sliders and editable text boxes for the user to enter the different mechanical parameters and applied force and torque. There are several menus in the interface to set the bar cross section thickness function, numerical parameters for Newton's method, and some examples for the user to begin familiarizing with the GUI.

After specifying all of these parameters, by pressing the button labeled "Run" (in gray), the GUI executes the computational module with all the specified parameters. After execution the GUI presents a graph of the resulting deformation. The two boxes on the GUI called "MN Iter" and "Relative Error" show the maximum number of iterations performed by Newton's Method and the approximate relative error on the computed solution. These two numbers can be used to assess the convergence or failure of it of the Newton iteration.

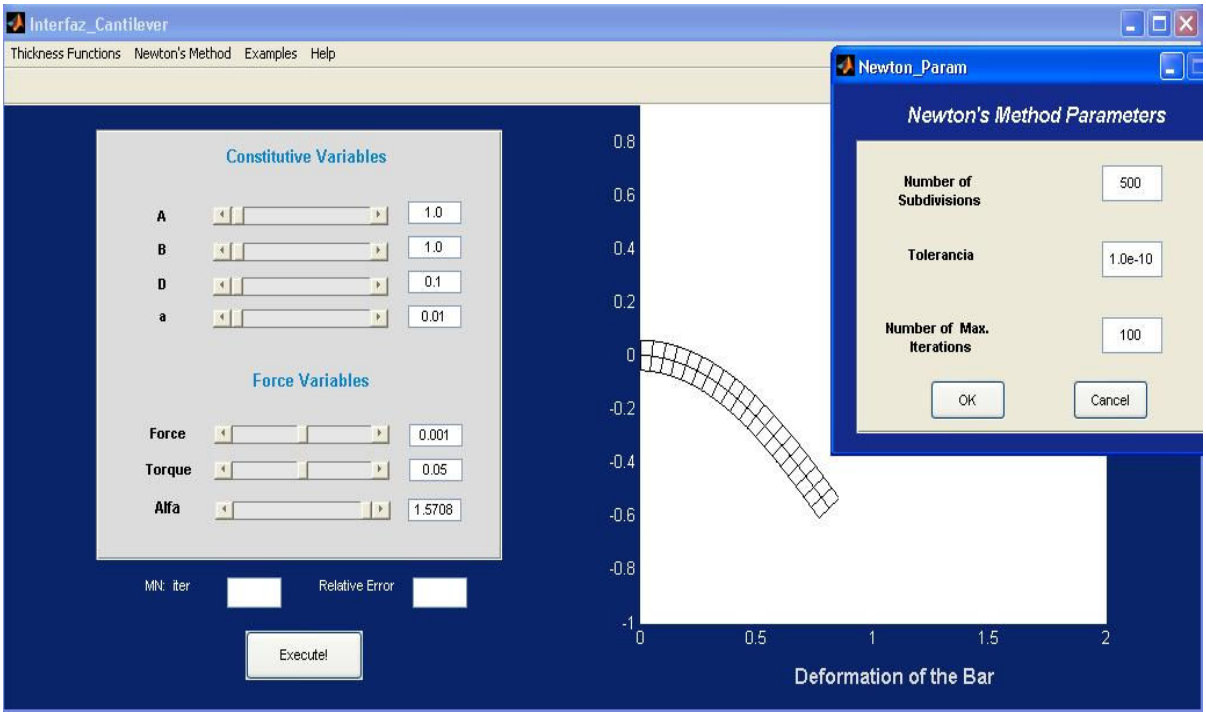

Figure 2: Snapshot of the graphical user interface for the cantilever problem.

5. Numerical Results

In this section we discuss some simulations corresponding to deformations of the nonlinear cantilever, using the GUI and method of Sections 3 and 4, respectively. The function $(EI)(s)$ in (8) was taken to correspond to a bar with circular cross sections and constant mass density. We used four different thickness functions: (1) constant, (2) linear decreasing (a bar thicker at the left end and thinner on the right end), (3) linear increasing (a bar thinner at the left end and thicker on the right end), and (4) quadratic (a bar thicker on both ends and thinner in the middle). The thickness functions were chosen in such a way that the individual total masses of the bars are equal.

In Figure 3 we show the corresponding line of centroids for the deformed bars corresponding to the different thickness functions that we described above. The values we used for the parameters in (8) and (9) are given by

$$A = 1, \quad B = 2, \quad a = 2, \quad D = 0.1, \quad \lambda = 0.0001, \quad \gamma = 0.01, \quad \alpha = \pi / 2. \tag{16}$$

One can see that the bar corresponding to the quadratic thickness function suffers the largest deflection: the thinner part in the middle makes it easier to bend this bar than the others. However, most of the deflection is concentrated on the right end of the bar. The linear decreasing suffers the least deflection. (This might explain why fishing rods are thicker on the handle and thinner on the other end.) Note that both the quadratic and linear decreasing thickness functions have very similar deflection close to the left end. The other two cases: constant and linear increasing are somewhat intermediate with the constant thickness suffering the least deflection. In Figure 4 we show the corresponding shear functions in each case. In all cases the largest shear is close to the left end. However, the linear decreasing thickness function has the least shearing close to the right side while the quadratic has the lowest shear close to the center of the bar where it is thinner.

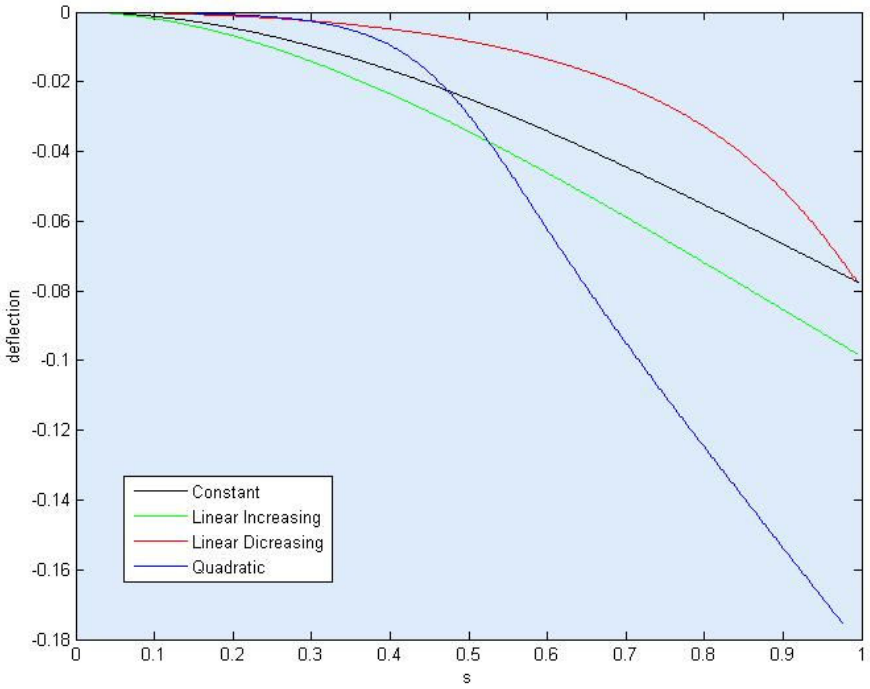

Figure 3: Curves of centroids for different thickness functions corresponding to the data (16).

In our next simulation, we fixed the thickness function to the linear decreasing and changed the shear parameter D in (8). The parameter values are like in (16) except for $\lambda = 0.001$, $\gamma = 0$. We see (Figure 5) that the smaller the value of D, the more shearable is the bar, with most of the shear towards the left end of the bar.

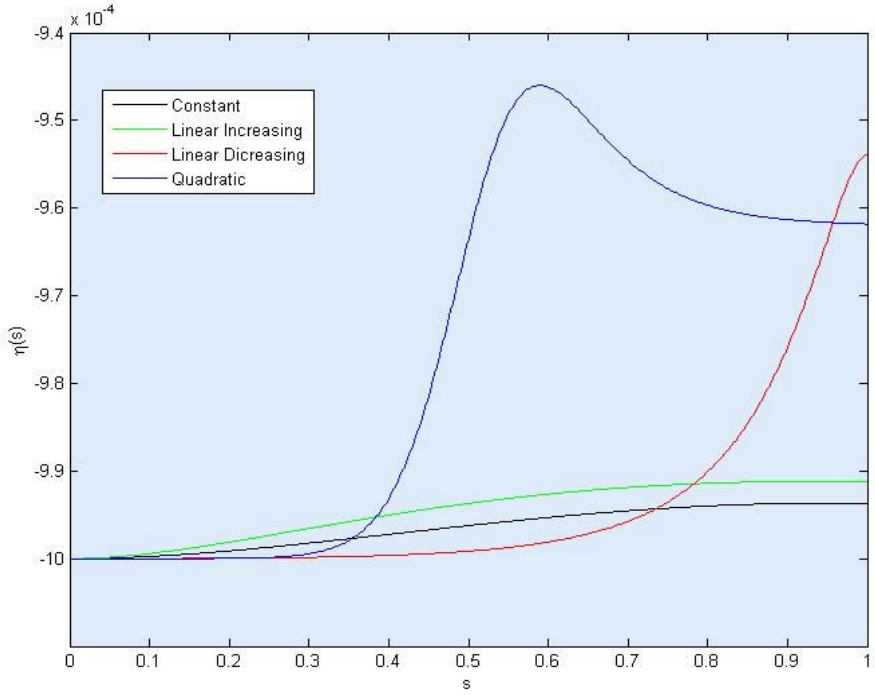

Figure 4: Shear functions for different thickness functions corresponding to the data (16).

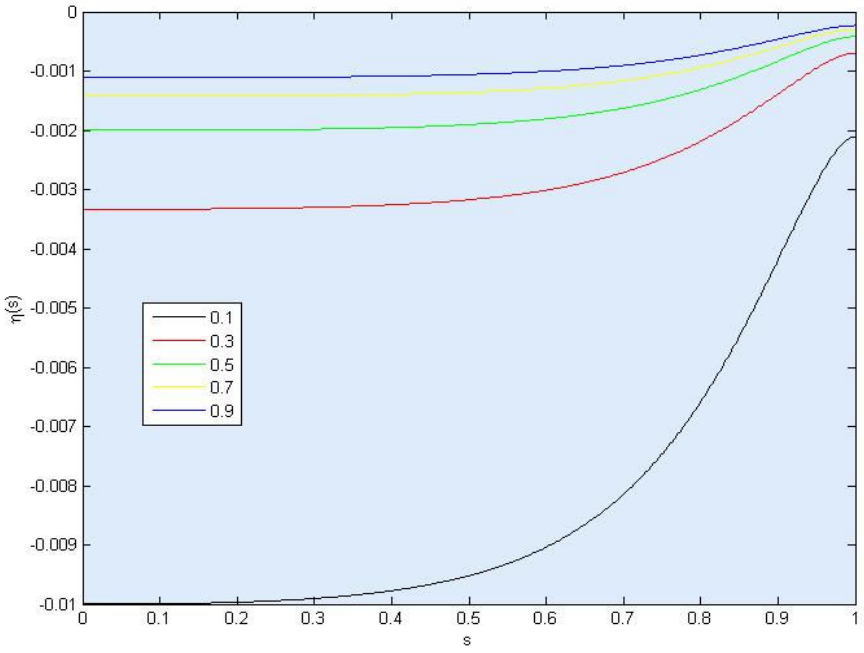

Figure 5: The function η(s) corresponding to different values of the shear parameter D.

6. Conclusions

The proposed numerical scheme and model for the nonlinear cantilever can be used to study the interactions of the various parameters describing the different constitutive and mechanical aspects of this problem. Even for the simple constitutive functions (8), the interrelation among the strains $\nu(s), \eta(s), \mu(s)$ is nonlinear. In a future work we will consider more general constitutive functions depending each of them on all the strains and to correlate the values of the different parameters in the model to actual laboratory data.

Nonlinear models of cantilevers are very common in the literature. Our model differs from many of these other problems either by the type of constitutive equations used or by the corresponding boundary conditions. For example, if we set $\nu = 1, \eta = 0$ in (1), $\mathbf{f}(s) = -q\mathbf{i}, \mathbf{l}(\mathbf{s}) = \mathbf{0}$ in (2) where q is a constant, $(EI)(s)$ equal to a constant in (8), and the boundary condition $\mathbf{n}(1) = \mathbf{0}$, then our equations reduce to the one considered in (6). The emphasis in this paper is on finding analytical asymptotic approximations to the solutions of the corresponding equations. On the other hand in (7) and (8) the deformations of the cantilever are modeled by describing the displacement of the free end of the bar using a forced mass-spring system with friction. The corresponding problems are time dependent (ours is static). The source of the nonlinearities comes from the form of the external or applied force, which is given by an electrostatic force with variable voltage, or by nonlinear (cubic) spring responses[8]. In (7) the dynamics of a single cantilever is studied, with results on the stability of solutions and Hopf bifurcations. In (8) the authors studied a lattice of cantilevers with up to six neighbor interactions and nonlinear spring responses.

7. Acknowledgments

This research has been funded in part by the National Security Agency, Grant Num. H98230-07-1-0114 and the NIH-RISE Program at the University of Puerto Rico at Humacao.

8. References

1. Stuart S. Antman, Nonlinear Problems of Elasticity, *Applied Mathematical Sciences 108*, xviii, Springer-Verlag, New York, 1995.

2. Kendall E. Atkinson, *An Introduction to Numerical Analysis*, 2nd edition, John Wiley & Sons, Inc, 1989.

3. Philip A. Yuya, Yongkui Wen, Joseph A. Turner, Yuris A. Dzenis, and Zheng Li, "Determination of Young's modulus of individual electrospun nanofibers by microcantilever vibration method", *Appl. Phys. Lett*. 90, 111909 (2007), DOI:10.1063/1.2713128.

4. H. Cui,', S. V. Kalinin,, X. Yang, and, D. H. Lowndes, "Growth of Carbon Nanofibers on Tipless Cantilevers for High Resolution Topography and Magnetic Force Imaging", Nano Letters **2004** 4 (11), 2157-2161.

5. Introduction to Elasticity-Wikiversity, http://en.wikiversity.org/wiki/Introduction_to_Elasticity.

6. P. N. Andriotaki, I. H. Stampouloglou, and E. E. Theotokoglou, "Nonlinear asymptotic analysis in elastica of straight bars – analytical parametric solutions, *Arch. Appl. Mech.*, (2006) 76: 525-536, DOI 10.1007/s00419-006-0054-4.

7. S. Liu, A. Davidson, and Q. Lin, Simulation studies on nonlinear dynamics and chaos in a MEMS cantilever control system, Journal of Micromechanics and Microengineering, 14 (2004) 1064-1073.

8. M. Sato, B. E. Hubbard, A. J. Sievers, B. Ilic, and H. G. Craighead, Europhysics Letters, 66 (3), pp. 318-323 (2004), DOI 10.1209/epl/i2003-10224-x.